Electronic Supplementary Material (ESI) for New Journal of Chemistry.

Supporting Information

Fabrication of Ag Nanoparticles Supported on One-Dimensional (1D) Mn_3O_4 Spinel Nanorods for Selective Oxidation of Cyclohexane at RoomTemperature

Shankha Shubhra Acharyya, Shilpi Ghosh, Sachin Kumar Sharma and Rajaram Bal*

Catalytic Conversion & Processes Division, CSIR-Indian Institute of Petroleum, Dehradun-248005, India. Fax: +91 135 2660202; Tel: +91135 2525 917; E-mail: raja@iip.res.in

Characterization Techniques. Powder X-ray diffraction spectra (XRD) were collected on a Bruker D8 advance X-ray diffractometer fitted with a Lynx eye high-speed strip detector and a Cu K_α radiation source. Diffraction patterns in the 2°-80° region were recorded at a rate of 0.5 degrees (2q) per minute. Scanning electron microscopy (SEM) images were taken on a FEI Quanta 200 F, using tungsten filament doped with lanthanumhexaboride (LaB_6) as an X-ray source, fitted with an ETD detector with high vacuum mode using secondary electrons and an acceleration tension of 10 or 30 kV. Samples were analyzed by spreading them on a carbon tape. Energy dispersive X-ray spectroscopy (EDX) was used in connection with SEM for the elemental analysis. The elemental mapping was also collected with the same spectrophotometer. Transmission electron microscopy (TEM) images were collected using a JEOL JEM 2100 microscope, and samples were prepared by mounting an ethanol-dispersed sample on a lacey carbon Formvar coated Cu grid. X-ray photoelectron spectroscopy (XPS) spectra were recorded on a Thermo Scientific K-Alpha X-Ray photoelectron spectrometer and binding energies (±0.1 eV) were determined with respect to the position C 1s peak at 284.8 eV. Chemical analyses of the metallic constituents were carried out by Inductively Coupled Plasma Atomic Emission Spectrometer; model: PS 3000 uv, (DRE), Leeman Labs, Inc, (USA). Fourier transform infra-red spectroscopy (FT-IR): The FTIR spectra were recorded on a Thermo Nicolet 8700 (USA) instrument with the operating conditions: resolution: 4 cm^{-1}, scan: 36, operating temperature: 23-25 °C and the frequency range: 4000-400 cm^{-1}. Raman spectra was measured at 298K by using a Laser Raman Spectrometer (JASCO, NRS-3100) with the 532 nm line from a diode-pumped solid-state laser for excitation.

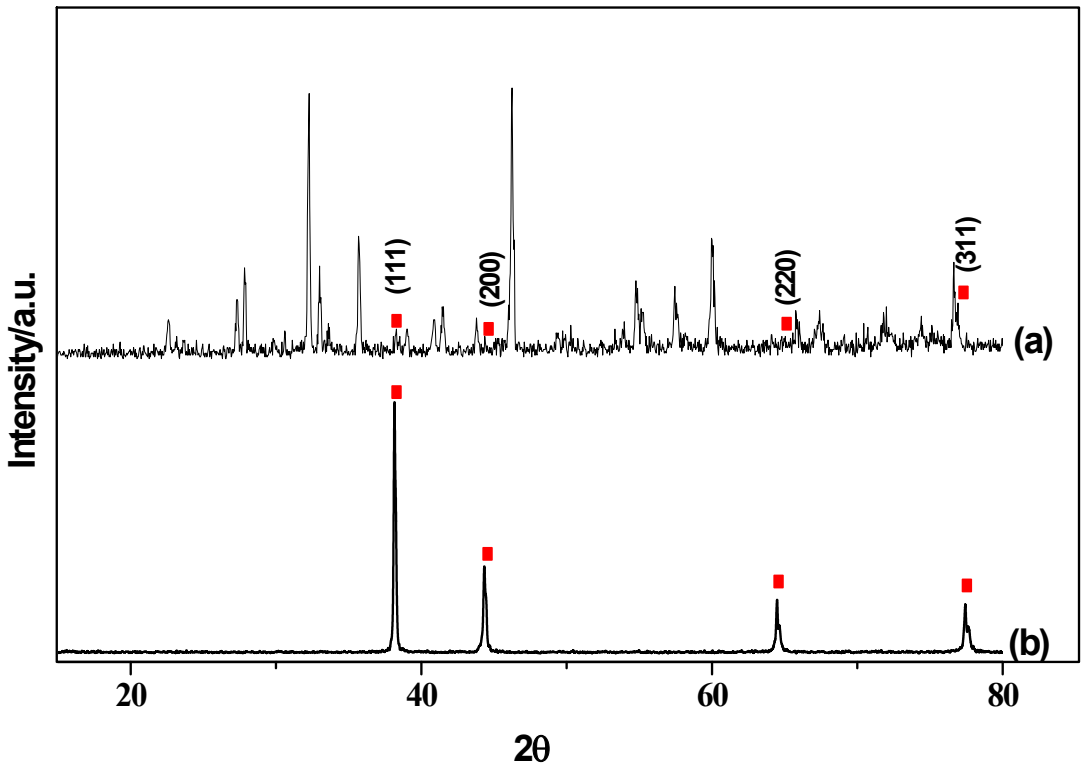

Figure S1. XRD of (a) Ag/Mn_3O_4 catalyst with Ag loading 7.8% and (b) that of commercial Ag.

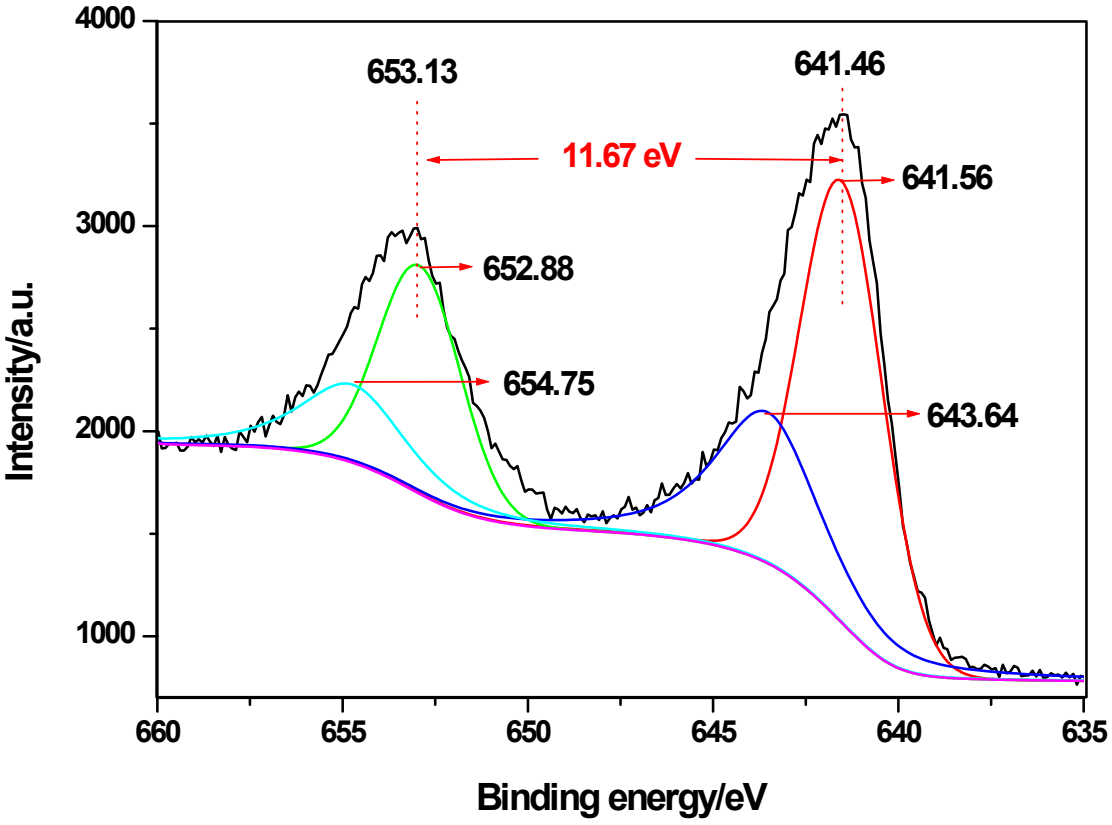

Figure S2. Mn 2p core-level spectra (XPS) of Ag-Mn nano-rod catalyst.

Table S1.

Mn-Species	Corresponding BE (eV)	Corresponding area (after deconvolution)
Mn^{3+} $2p_{3/2}$	641.56	3937.18
Mn^{2+} $2p_{3/2}$	643.64	2095.7
Mn^{3+} $2p_{1/2}$	652.88	2985.2
Mn^{2+} $2p_{1/2}$	654.75	1900.0

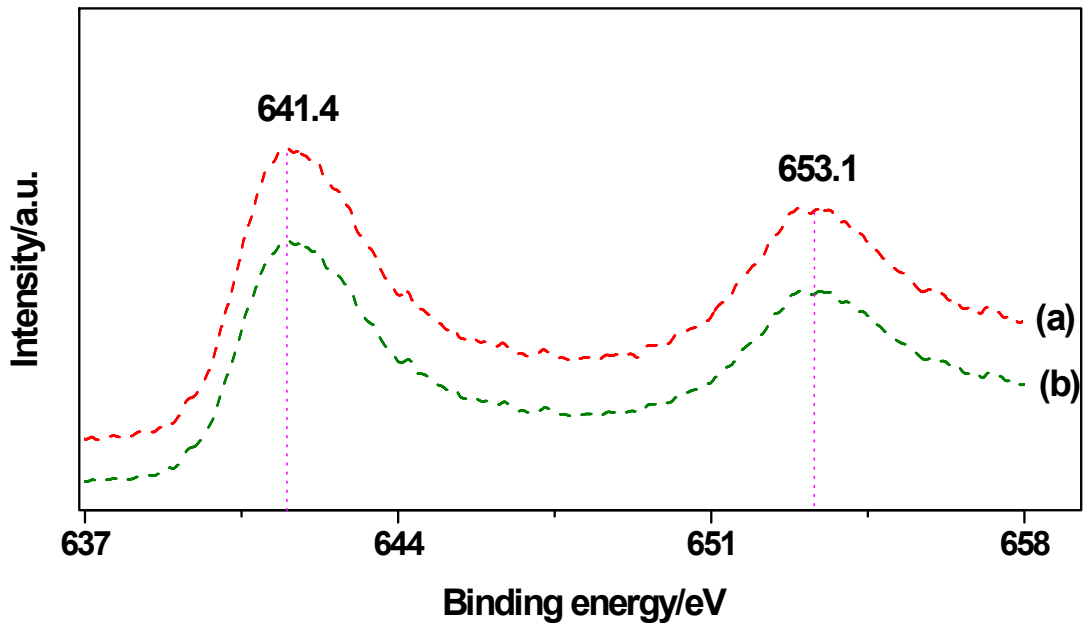

Figure S3. Mn 2p core-level spectra (XPS) of (a) fresh and (b) spent Ag-Mn nano-rod catalyst.

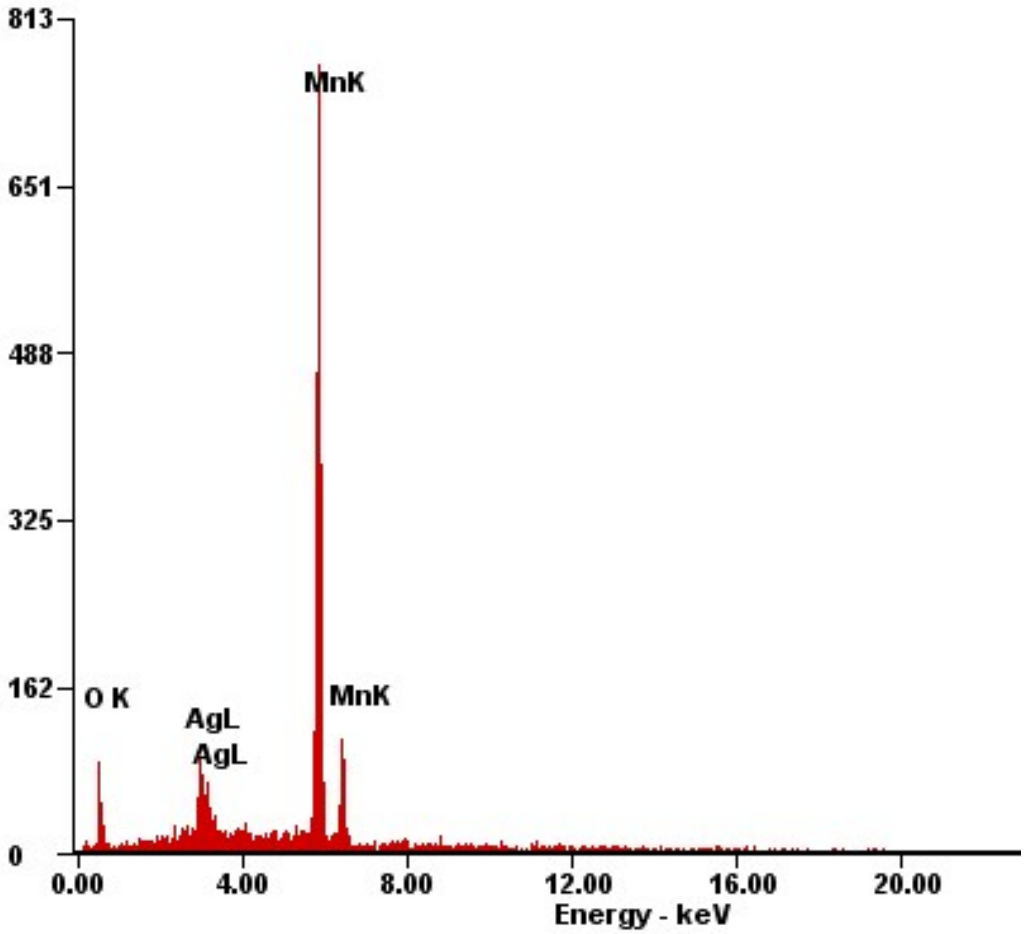

Figure S4. SEM-EDAX of the Ag-Mn nano-rod catalyst.

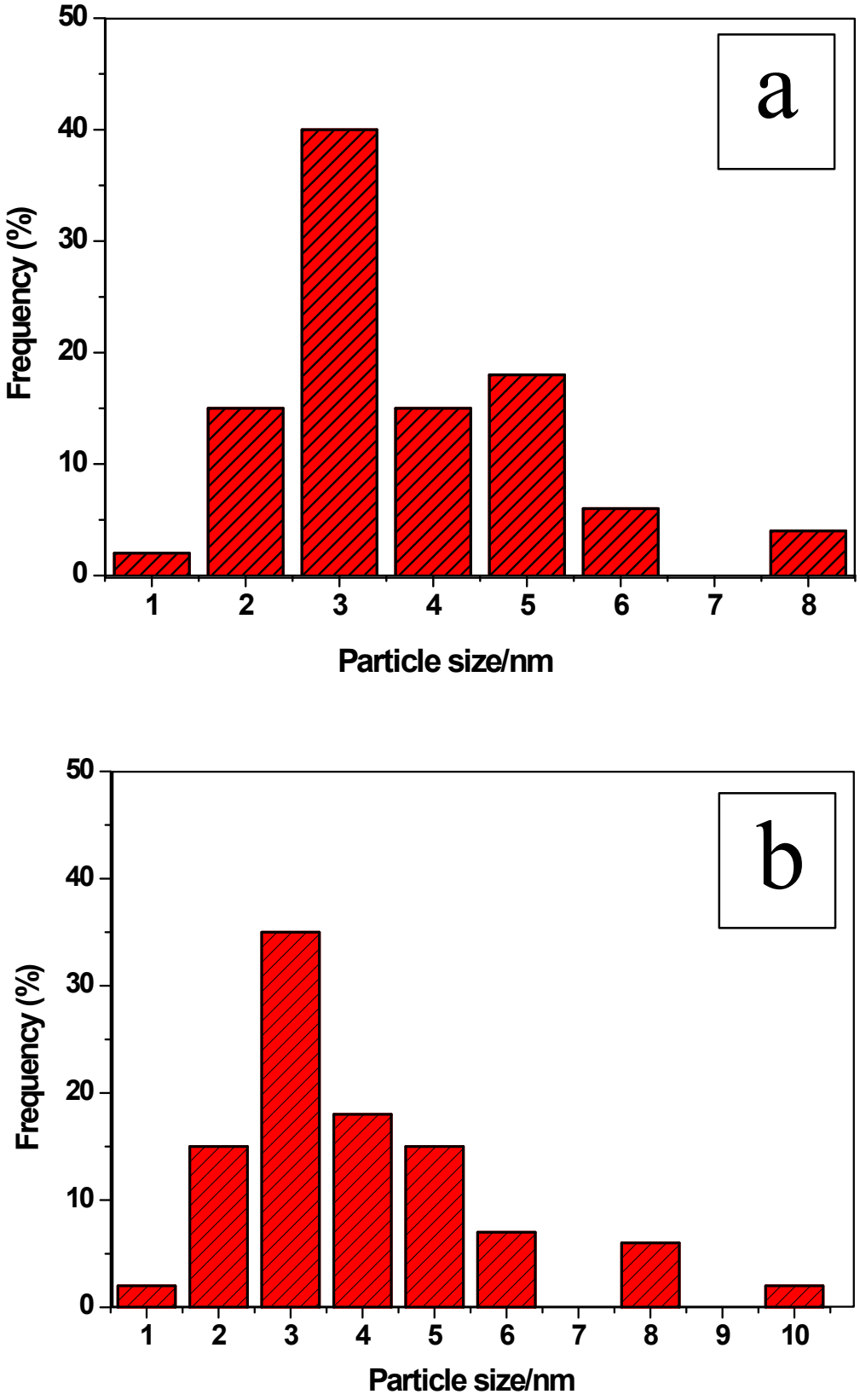

Figure S5. Particle size distributions (histogram) of fresh catalyst (based on TEM diagram Figure 6e) and (b) that of spent catalyst (based on Figure 6f).

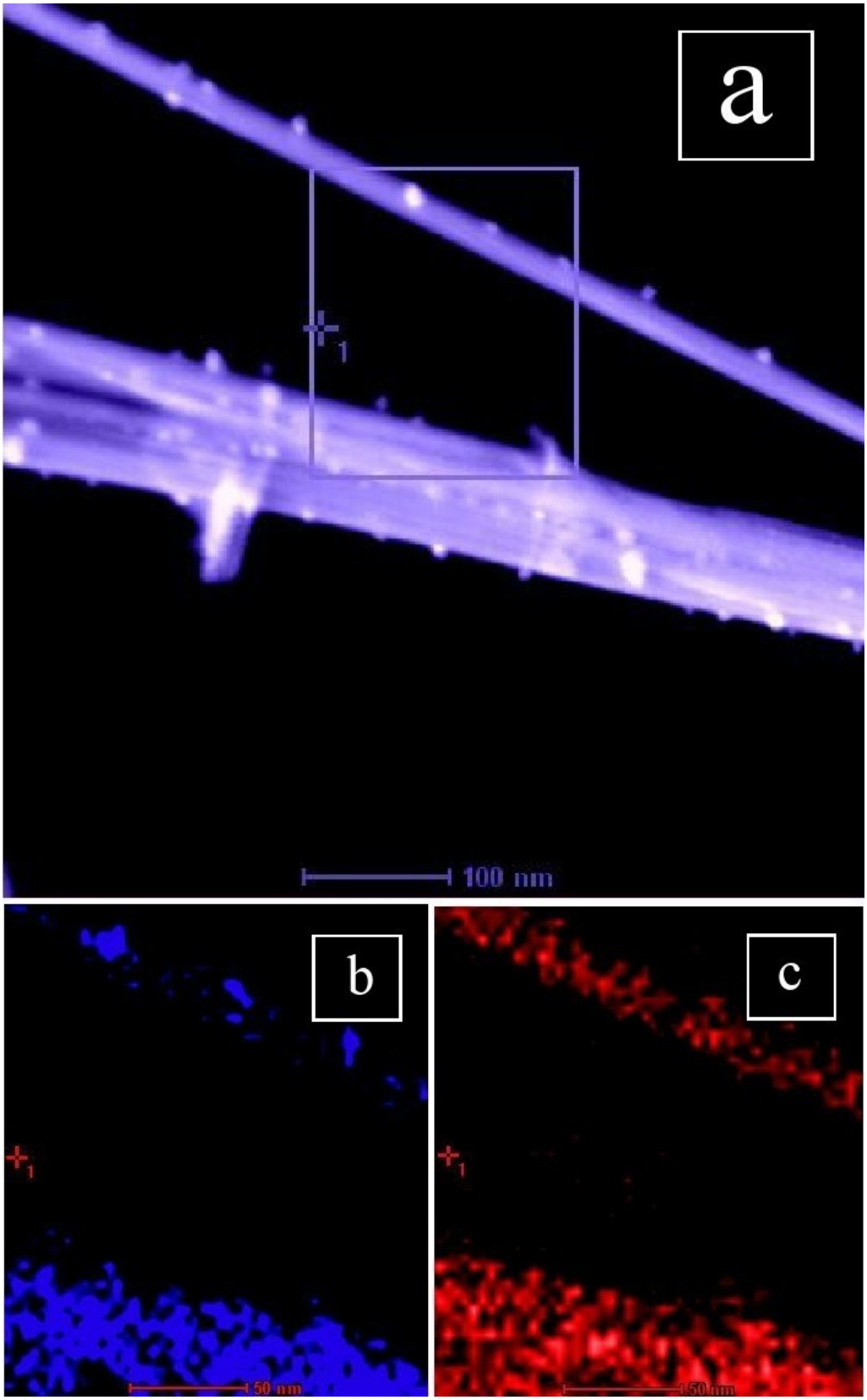

Figure S6. STEM-Elemental mapping of (b) Ag, (c) Mn and (d) O based on Figure 4a (Main) Ag-Mn nano-rod catalyst.

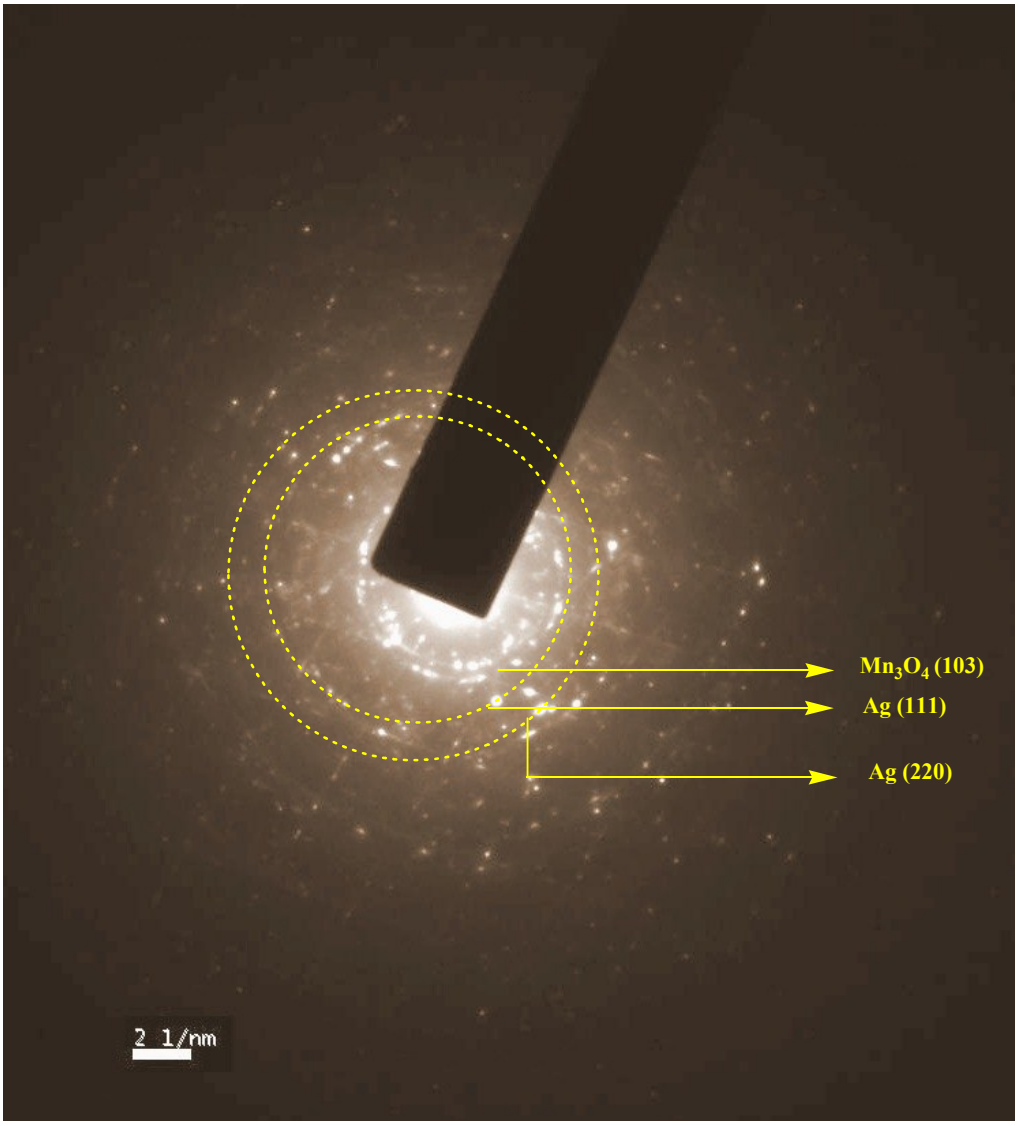

Figure S7. TEM-SAED of the Ag-Mn nano-rod catalyst.

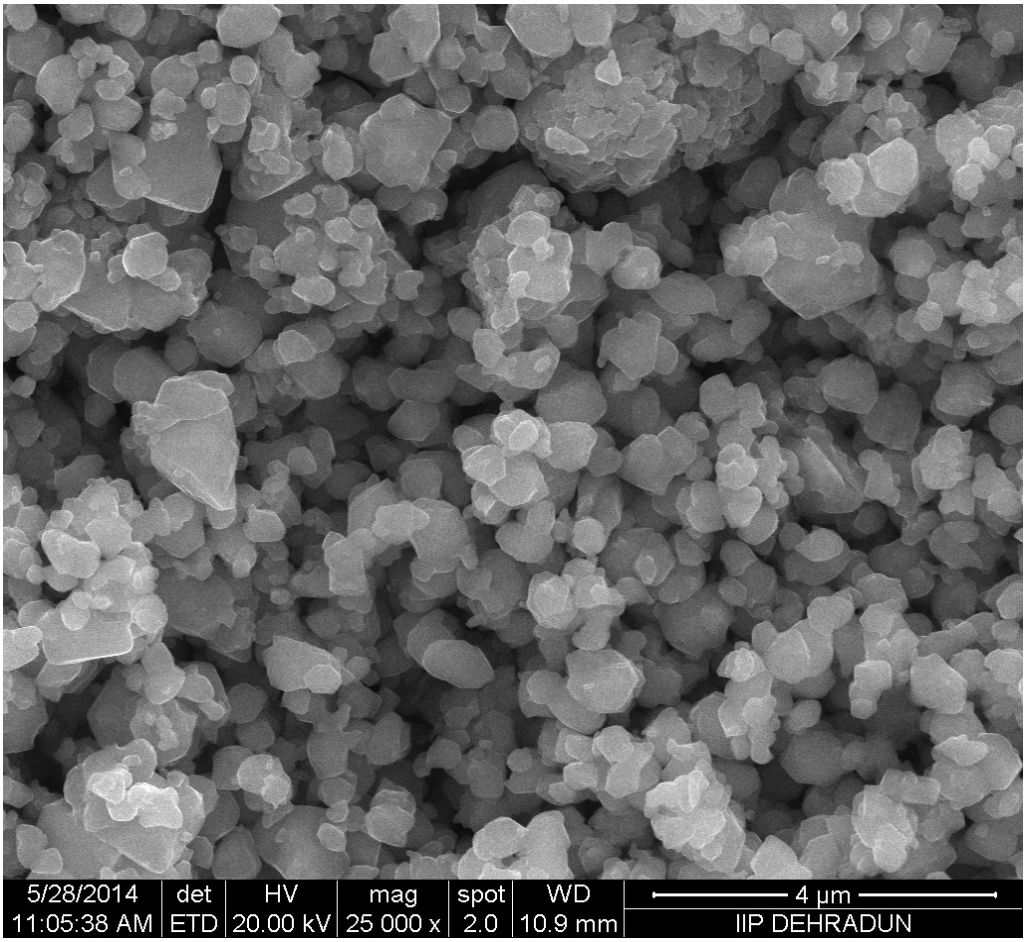

Figure S8. SEM image of the Ag-Mn sample without using CTAB.

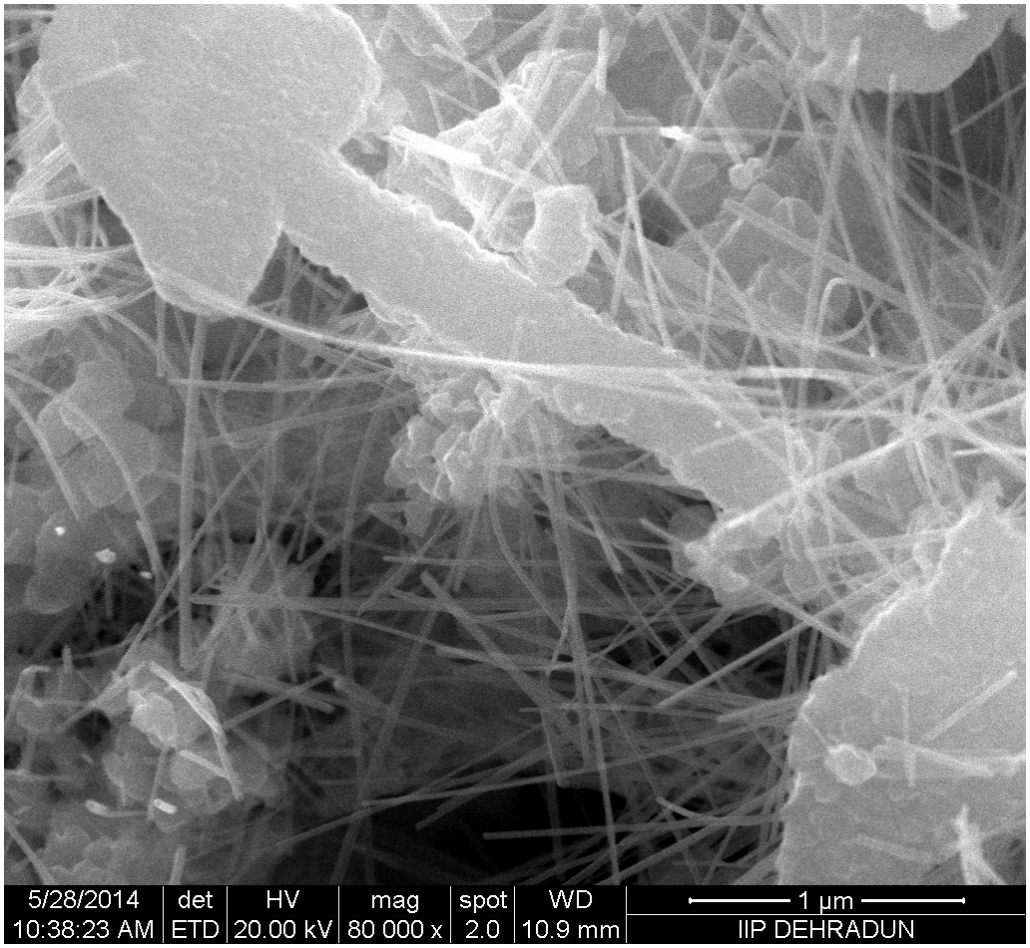

Figure S9. SEM image of the Ag-Mn sample when Ag: CTAB molar ratio was 1:1.

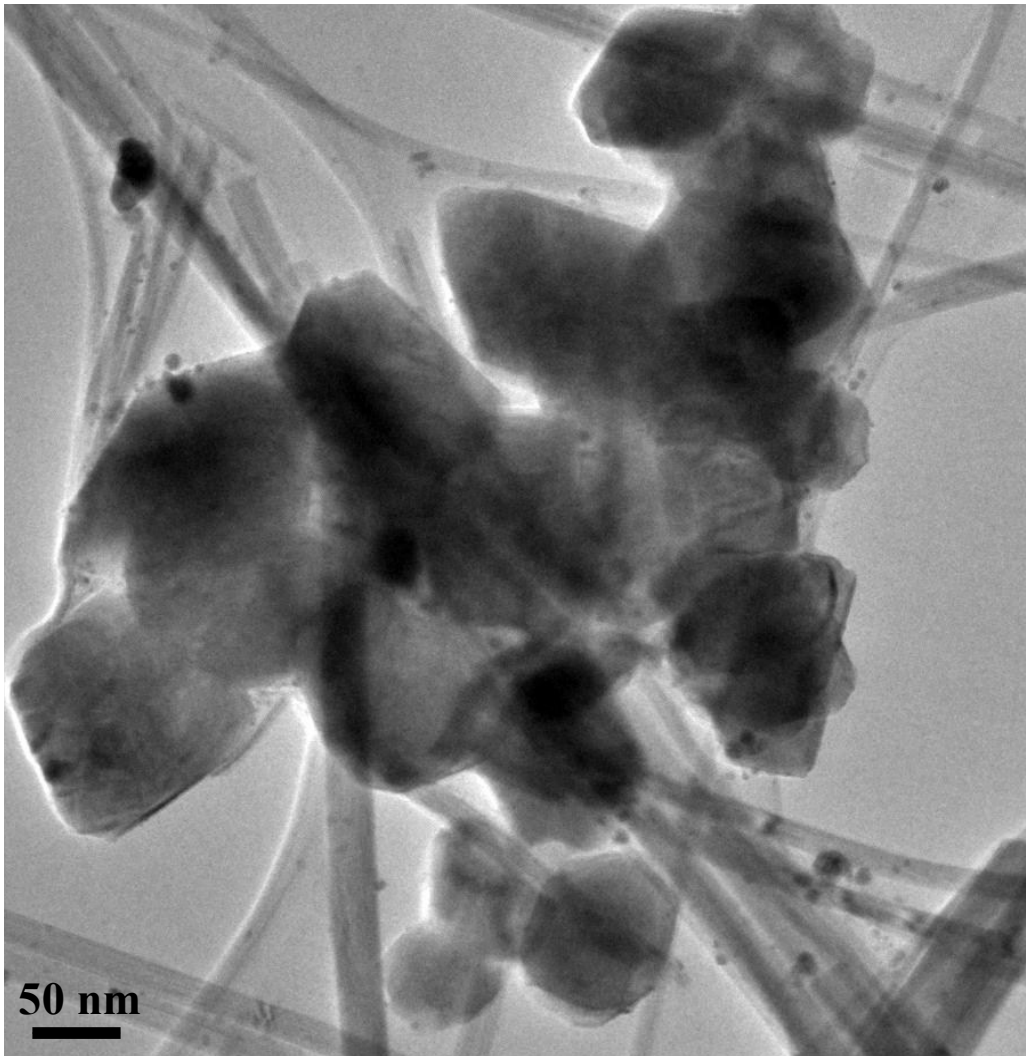

Figure S10. TEM image of the Ag-Mn sample when the hydrothermal treatment time was 6h.

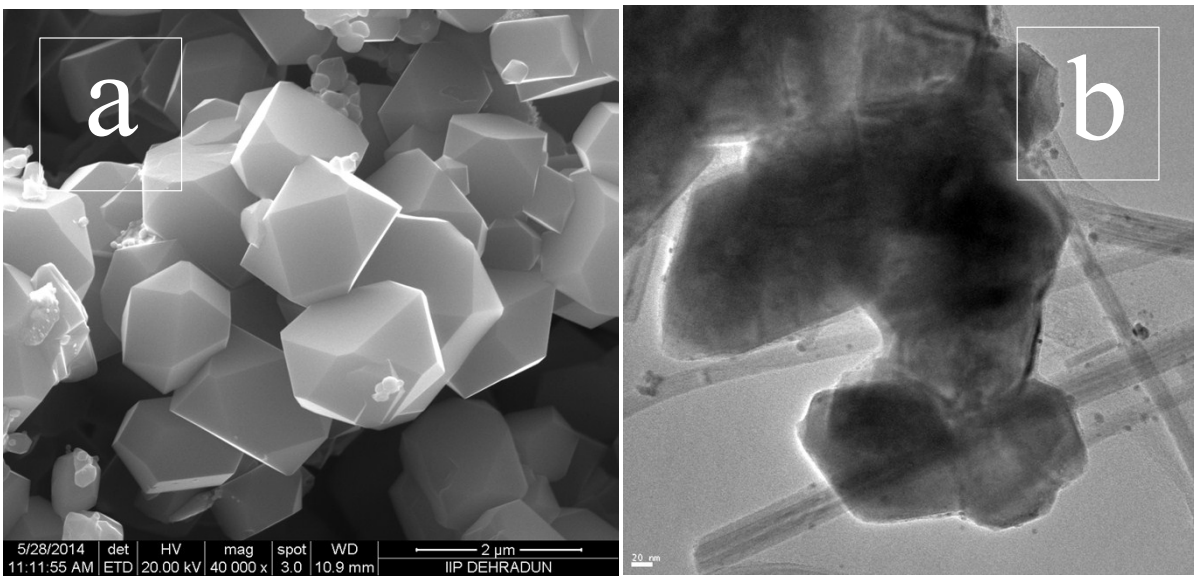

Figure S11. (a) SEM and (b) TEM images of the Ag-Mn sample when the hydrothermal treatment time was prolonged to 30h.

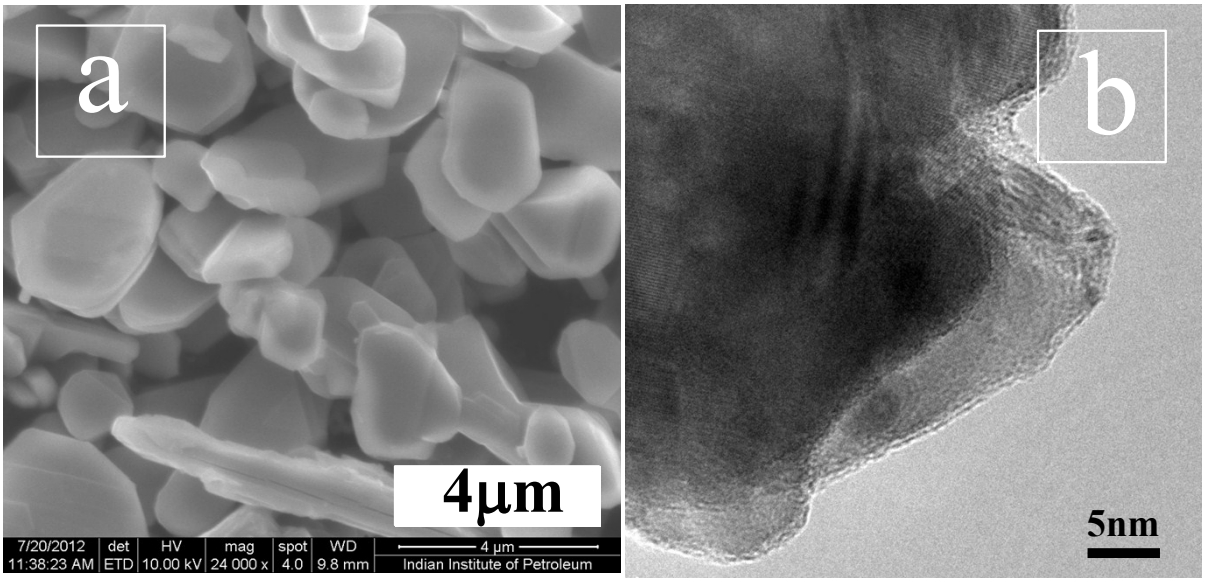

Figure S12. (a) SEM and (b) TEM images of the Ag-Mn sample when $KMnO_4$ was used as precursor of Mn.

Table S2. Comparative study of catalytic activities of different catalyst in cyclohexane oxidation

Entry	Catalyst	Oxidant	Temp (°C)	Time (h)	C_B (%)	S_P (%)	Ref.
1	CoAlPO-36	O_2/pressure (air) = 1.5 MPa.	130 °C	16h	19.05	62.6	(1)
2	Calcined vanadium phosphorus oxide (VPO)	H_2O_2	65 °C	20h	96	50	(2)
3	Ionic liquid, 1-butyl-3-methylimidazolium tetrafluroborate (BmimBF4) template-assisted synthesized boron and fluorine-enriched mesoporous polymeric carbon nitride.	H_2O_2	150 °C	4h	7.8	91	(3)
4	Carbon Nanotubes	O_2/pressure (air) = 1.5 MPa.	125 °C,	8 h	34.3	22	(4)
5	Cr-MIL-101 (Metal-organic framework)	TBHP+O_2	70 °C	8h	8	81	(5)
6	Cu-nanoclustures supported on nanocrystalline Cr_2O_3	H_2O_2	40 ºC	3h	86	85	(6)
7	Hemicryptophane copper complex	H_2O_2	35 °C	2h	31	95	(7)
8	Gold nanoparticles supported on carbon materials	H_2O_2	RT	6h	3.6	99	(8)
9	Gold(III) complexes of type $[AuCl_2\{\eta2\text{-}RC(R'pz)3\}]Cl$ [R = R' =H(1),R=CH2OH, R' =H(2) and R = H, R' = 3,5-Me (3), pz = pyrazol-1-yl] were supported on carbon materials oxidised with nitric acid (-Oxi) or oxidised with nitric acid and subsequently treated with sodium hydroxide	H_2O_2	RT		Yield =7.2%		(9)
10	MTIX [M= Cr and V; X=0,5,10,20%)	TBHP	70 °C	6h	35	92	(11)
11	$CuCr_2O_4$ nanoparticles	H_2O_2	50 °C	10 h	70	85	(12)
12	[(MoV/MoVI)mO]n	O_2/pressure (air) = 0.3 MPa.	140 °C,	17h	6	40	(13)

13	**Ultrasmall Ag nanoparticles supported on Mn_3O_4 1D nanorods**	**H_2O_2**	**40 °C**	**10**	**88**	**75**	**This work**

References

(1) G. Sankar, R. Raja and J. M. Thomas, *Catal. Letters,* 1998, **55***,* 15–23.

(2) U. R. Pillai and E. Sahle-Demessie, *New J. Chem.,* 2003, **27**, 525–528.

(3) Y. Wang, J. Zhang, X. Wang and M. Antonietti, *Angew. Chem.,* 2010, **49,** 3356 –3359.

(4) H. Yu, F. Peng, J. Tan, X. Hu, H. Wang, J. Yang and W. Zheng, *Angew. Chem.,* 2011, **123**, 4064 – 4068.

(5) N. V. Maksimchuk, K. A. Kovalenko, V. P. Fedin and O. A. Kholdeeva, *Chem. Commun.,* 2012, **48***,* 6812–6814.

(6) B. Sarkar, P. Prajapati, R. Tiwari, R. Tiwari, S. Ghosh, S. S. Acharyya, C. Pendem, R. K. Singha, L. N. S. Konathala, J. Kumar, T. Sasaki and R. Bal, *Green Chem.,* 2012, **14**, 2600–2606.

(7) O. Perraud, A. B. Sorokin, J. P. Dutasta and A. Martinez, *Chem. Commun.,* 2013, **49***,* 1288–1290.

(8) S. A. C. Carabineiro, L. M. D. R. S. Martins, M. Avalos-Borja, J. G. Buijnsters, A. J. L. Pombeiro and J. L. Figueiredo, *Appl. Catal. A: Gen*, 2013, **467,** 279–290

(9) M. Peixoto de Almeida, L. M. D. R. S. Martins, S. A. C. Carabineiro, T. Lauterbach, F. Rominger, A. S. K. Hashmi, A. J. L. Pombeiro and J. L. Figueiredo, *Catal. Sci. Technol.,* 2013, **3**, 3056–3069.

(10) A. Bellifa, A. Choukchou-Braham, C. Kappenstein and L. Pirault-Roy, *RSC Adv.***,** 2014, **4**, 22374–22379.

(11) S. S. Acharyya, S. Ghosh, S. Adak, D. Tripathi and R. Bal, *Catal. Commun.,* 2015, **59,** 145–150.

(12) X. Liu, M. Conte, W. Weng, Q. He, R. L. Jenkins, M. Watanabe, D. J. Morgan, D. W. Knight, D. M. Murphy, K. Whiston, C. J. Kiely and G. J. Hutchings, *Catal. Sci. Technol.,* 2015, **5**, 217–227.